# Effect of Short Chain-Branching Distribution on Crystallinity and Modulus of Metallocene-Based Ethylene–Butene Copolymers

XURONG XU,[1]* JUNTING XU,[1] LINXIAN FENG,[1] WEI CHEN[2]

[1] Department of Polymer Science & Engineering, Zhejiang University, Hangzhou 310027, People's Republic of China

[2] Research Institute of Petroleum Processing, SINOPEC, Beijing 100083, People's Republic of China

*Received 5 March 1999; accepted 19 August 1999*

**ABSTRACT:** In this article, the short chain-branching distribution (SCBD) of some metallocene-based ethylene–butene copolymers was evaluated by DSC, and some conventional ethylene copolymers were also studied for the purpose of comparison. It is found that metallocene-based ethylene copolymers have a relative narrower SCBD. These copolymers were crystallized under different modes, and the crystallinity and initial modulus of them were examined. The metallocene-based ethylene copolymers contain less interfacial regions, and the melting temperatures of them decrease more rapidly with the decrease of density than those of conventional ethylene copolymers. Moreover, the metallocene-based and conventional ethylene copolymers of similar density have close initial modulus when they are quenched or annealed at 100°C, but conventional ethylene copolymers show higher initial modulus when stepwise crystallized from 120°C. These differences in crystallinity and initial modulus were explained based on their differences in short-chain branching distributions. © 2000 John Wiley & Sons, Inc. J Appl Polym Sci 77: 1709–1715, 2000

**Key words:** short-chain branching distribution (SCBD); ethylene–butene copolymers

## INTRODUCTION

Short chain-branched ethylene-$\alpha$-olefin copolymers are among the most widely applied plastics. By varying the content of comonomer, different copolymers, from high-density polyethylene (HDPE) to linear low-density polyethylene (LLDPE), even ultralow-density polyethylene (ULDPE) can be obtained. The mechanical properties of ethylene copolymers depend on many factors, such as molecular structures[1–4] (composition, composition distribution, molecular weight, molecular weight distribution, etc.) and supermolecular structures[5–7] (morphology, crystallinity, entanglements, etc.). The ethylene copolymers produce by conventional heterogeneous Ziegler-Natta catalysts usually show broad composition and molecular weight distributions due to the presence of multiple active sites, and the microstructure of the obtained polymer chains is uncontrollable. This makes it difficult to determine the effect of various factors on mechanical properties of ethylene copolymers.

Copolymerization of ethylene with $\alpha$-olefins using Kaminsky-type metallocene catalysts, which are generally believed to have "single site", can yields copolymers with homogeneous composition

* *Present address:* Department of Polymer Science and Engineering, Peking University, Beijing 100871.

*Correspondence to:* J. Xu.

Contract grant sponsor: National Natural Science Foundation of China; contract grant sponsor: 5970 3002.

Contract grant sponsor: State Key Laboratory of Polymeric Materials Engineering, CUST.

Journal of Applied Polymer Science, Vol. 77, 1709–1715 (2000)

**Table I Characteristics of Samples**

| Samples | Comonomer Content (mol %) | Density[a] (g/cm$^3$) | $M_w$ ($\times 10^{-4}$) | $M_w/M_n$ |
|---|---|---|---|---|
| MPE1 | 0.38 | 0.947 | 11.10 | 2.28 |
| MPE2 | 0.87 | 0.940 | 15.49 | 3.80 |
| MPE3 | 1.16 | 0.931 | 8.01 | 2.72 |
| ZNPE1 | 0.58 | 0.949 | 13.86 | 6.49 |
| ZNPE2 | 4.45 | 0.920 | 14.12 | 4.33 |

[a] Density of as-received samples.

distribution and a narrow molecular weight distribution around 2.0.[8,9] This provides an opportunity to investigate the mechanical properties of ethylene copolymers with narrow composition distribution, and also facilitates study of the roles of short chain branching and short chain-branching distribution (SCBD) in the mechanical properties of ethylene copolymers.

Temperature-rising elution fractionation (TREF) technique is usually applied to obtain the SCBD of ethylene copolymers, but differential scanning calorimeter (DSC) is also used to evaluate the SCBD of ethylene copolymers,[10] because DSC traces reflect the lamella crystal thickness distribution, which is related with SCBD.[11] The fractionation by DSC is based on the same principle of separation as TREF, though it does not physically separate the fractions.[12] However, because some short chain branches can be incorporated into the crystalline lattice, especially for melt-quenched PE, the lamella crystal thickness distribution is different from SCBD to some extent.[13,14] Therefore, to evaluate the SCBD by DSC, the treatment of samples is very important. When samples were continuously cooled from melting state at a very slow rate (1.5°C/h) or treated with the stepwise crystallization method, the obtained result was comparable to that of TREF.[15,16]

In the present work, the SCBDs of some metallocene-based and Ziegler-Natta catalyst-based ethylene copolymers were evaluated by means of DSC. And the effect of the SCBDs of ethylene copolymers on thermal properties, crystallinity, and initial modulus were investigated under different crystallization conditions.

## EXPERIMENTAL

### Materials

Three ethylene–butene copolymer samples (MPE1, MPE2, and MPE3) prepared with metallocene catalyst were supplied by RIPP, SINOPEC. Two commercial ethylene–butene copolymer samples, ZNPE1 and ZNPE2, prepared with a conventional Ziegler-Natta catalyst, were commercial products of Qilu Petrochemical Co. in China. Some characteristics of these samples are listed in Table I. The selected samples have close molecular weight (except for MPE3).

### Treatment of Samples

Specimens of each polymer were prepared by compression molding, followed by a predetermined thermal treatment. About 50 g of copolymer was placed on a 20 × 20 cm, 2.0 mm-thick mold that was positioned between two cooper plates. Samples were kept at 170°C for 20 min under the applied pressure of 150 kg/cm$^2$, then were followed by three different heat treatments: (1) quickly quenched with ice water; (2) quickly transferred into an oil bath of 100°C and kept for 20 h under nitrogen gas atmosphere and then quenched with ice water; and (3) quickly transferred into an oil bath of 120°C. The temperature of the oil bath decreases stepwise, and at each temperature the samples were maintained for 12 h under nitrogen gas atmosphere. The temperatures of oil bath were 120, 115, 105, 100, 95, 90, 85, and 80°C, respectively.

### Characterization

The molecular weight and molecular weight distribution of ethylene copolymers were measured with Waters 150 GPC at 135°C using trichlorobenzene as the solvent.

The contents of short chain branching were determined by $^{13}$C-NMR spectra at 100.7 MHz recorded on a Bruker AMX-400 spectrometer at 370 K. The polymer solutions were prepared by dissolving ca. 50 mg polymer at 130°C in 0.5 mL $C_6D_4Cl_2$. One percent hexamethyldisiloxane (HMDS) was added as the internal standard. The

pulse angle was 90°, pulse repetition, 10 s, spectral width, 5000 Hz, number of scans, 6000, and data points, 32 K.

Densities of the ethylene copolymers were determined in a density gradient column, consisting of a water–isopropyl alcohol mixture, at a constant temperature of 22°C. The volume fraction crystallinity on a density basis, $\chi_v$, was calculated according to following equation:[7]

$$\chi_v = (\rho - \rho_a)/(\rho_c - \rho_a) \quad (1)$$

where $\rho_c$, $\rho_a$ are the density of the crystalline and amorphous regions with the values of 1.000 and 0.852 g/cm$^3$, respectively, which were given by Chiang and Flory.[18]

The weight fraction crystallinity, $\chi_d$, was calculated by:[17]

$$\chi_d = \rho_c\chi_v/(\rho_c\chi_v + \rho_a(1 - \chi_v)) \quad (2)$$

The DSC thermographs were recorded on a Perkin-Elmer differential scanning calorimeter (DSC-7), and the melting temperature and enthalpy were calibrated by standard substance indium at the same heating rate. The weight of ethylene copolymers for the DSC analysis was 2.0–3.0 mg. The samples were encapsulated into an aluminum pan, and were heated from room temperature to 160°C at a heating rate of 5°C/min. The weight fraction crystallinity based on fusion enthalpy, $\chi_{\Delta H}$, was calculated by comparison with the fusion enthalpy of a perfect crystalline polyethylene, i.e., 289 J/g.[19]

### Tensile Test

The force–elongation curves of the samples were recorded on an Instron Tensile Test Machine at a crosshead speed of 100 mm/min. The width and thickness of center part of the dumb bell-shaped samples for tensile test were 6.0 and 2.0 mm, respectively, according to Chinese standard GB/T 1040-92. All samples were tested at an ambient temperature 22°C. The distance between the cross heads was 25 mm. These dimensions were measured to an accuracy of 0.02 mm. The initial modulus, $E$, which is the stress divided by the strain at very low deformation levels, was calculated from the initial part of the stress–strain curve using a linear regression method.

## RESULT AND DISCUSSION

### Short-Chain Branching Distribution

Because the polymer chains contain a different amount of the comonomer and show the different crystallization temperatures, they will segregate when stepwise crystallized, leading to multiple melting peaks. The lower the comonomer content, the higher crystallization and melting temperature. Thus, from the number and intensity of melting peak and melting temperature range of stepwise crystallized ethylene copolymers one can compare the short chain-branching distribution of ethylene copolymers. Figure 1 shows the DSC melting traces of various samples after stepwise crystallization. Only one strong peak is observed in the melting curve of MPE1, indicating its relatively narrow SCBD. Some weak peaks besides a major peak also appear in the melting curves of MPE2 and MPE3. Likely, ZNPE1 also shows multiple melting peaks. However, the intensity of the lower peaks (i.e., other than the major peak) is stronger than that of MPE2 and MPE3, and it exhibits a wider melting temperature range. This suggests that ZNPE1 has a broader SCBD than MPE1, MPE2, and MPE3. ZNPE2 has the highest number of melting peak and the widest melting temperature range among these five samples, implying that this sample has the broadest SCBD. In the TREF curves of these ethylene copolymers, the number and intensity of peaks and elution temperature range show a similar variation to that of melting behavior.[20]

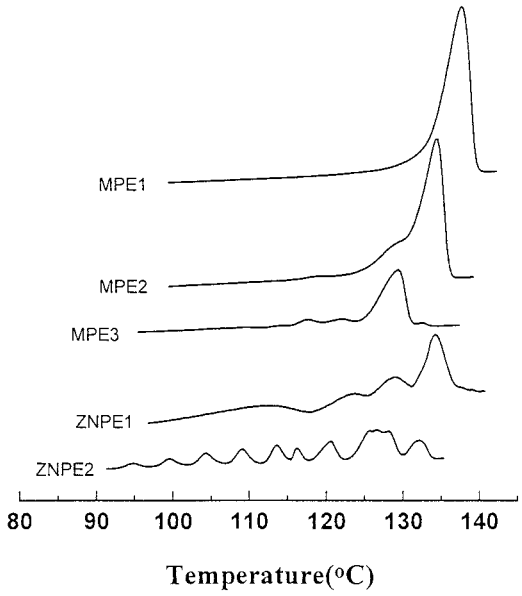


**Figure 1** DSC melting traces of stepwise crystallized samples.

### Melting Temperature

The variation of melting temperature of quenched samples and density of as-received samples with

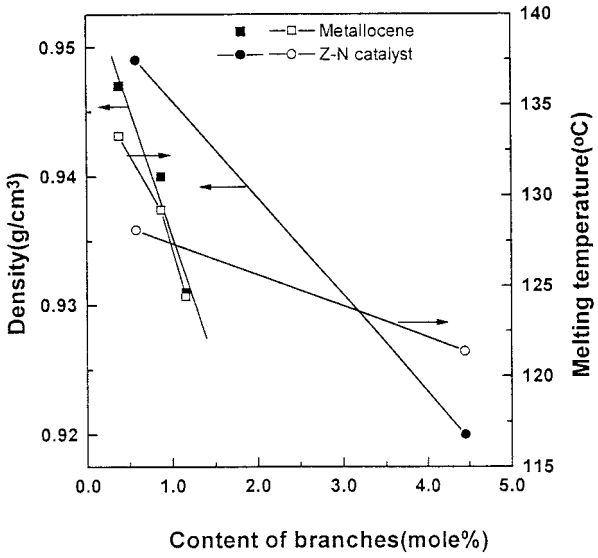


**Figure 2** The effect of comonomer content on melting temperature and density.

comonomer content is illustrated in Figure 2. The melting temperatures of all samples decrease with increasing in comonomer content. However, one can clearly see that metallocene-based samples (MPE1, MPE2, and MPE3) show lower melting temperatures than those of the Ziegler-Natta catalyst-based ones (ZNPE1 and ZNPE2) when they have a similar comonomer content. For the ethylene copolymers prepared with conventional Ziegler-Natta catalysts, the distribution of short branches among different polymer chains is not homogeneous.[21] The shorter polymer chains usually contain more comonomer units and show lower melting temperature, whereas the longer polymer chains tend to be less branched and exhibit a higher melting temperature,[22] while in the polymers having a narrower SCBD such as metallocene-based samples, various polymer chains have a close comonomer content. Because the melting temperature of a polymer is mainly determined by its fractions of high melting temperature, at the same comonomer level the polymer with a broader SCBD always shows a higher melting temperature than that with a narrower SCBD due to the presence of less branched fractions, in which the comonomer content is lower than that of the homogeneously branched polymer.

The short chain-branching distribution also has efficiency that comonomer units reduce the density and melting temperatures of polymers. It is observed from Figure 2 that the density and melting temperatures of metallocene-based polymers decrease much faster with increasing the comonomer units than those of conventional ethylene copolymers, indicating that copolymerization using a metallocene catalyst decrease the melting temperature of the polymer more efficiently. It is also found that the density and melting temperatures of metallocene-based copolymers decrease with increasing in comonomer content at a close rate, but the melting temperatures of conventional ethylene copolymers show a slower decrease rate than density. This is because less branched fractions always exist in the polymer having a broad SCBD, irrespectively of the comonomer content. As a result, in the melting temperatures of metallocene-based polymers decrease with density much faster than conventional ethylene copolymers (Fig. 3), as reported by Kashiwa.[23]

## Crystallinity

The degree of crystallinity is an important element of the phase structure. There are several methods to measure the degree of crystallinity of polymers. Although different methods of measurement display the same functional behavior, a detailed comparison shows that there are small but significant differences between techniques.[24] The crystallinity calculated from density are based on a two-phase model: the amorphous phase and the crystalline phase. However, evi-

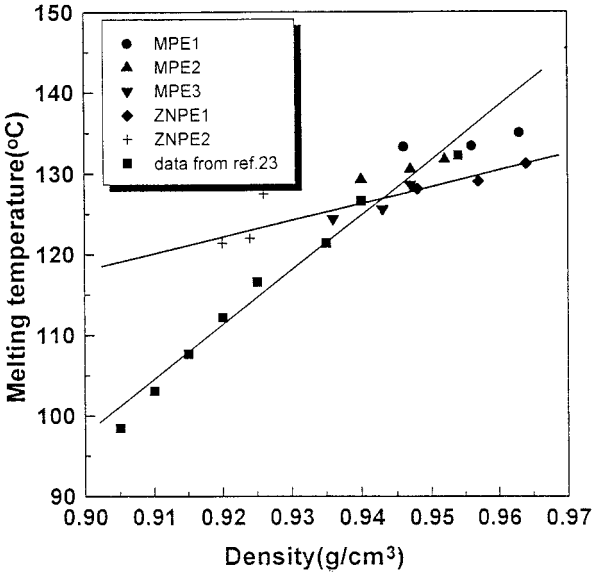


**Figure 3** The relationship between melting temperature and density.

**Table II Crystallinity and Some Related Data for Different Samples**

| Sample | Crystallization Procedure | Density (g/cm$^3$) | $T_m$[a] (°C) | $\chi_d$ (%) | $\chi_{\Delta H}$ (%) | $\alpha_i$ (%) | $E$ (MPa) |
|---|---|---|---|---|---|---|---|
| | I | 0.946 | 133.3 | 67 | 58 | 9 | 934 |
| MPE1 | II | 0.956 | 133.4 | 73 | 64 | 9 | 1161 |
| | III | 0.963 | 135.0 | 78 | 68 | 10 | 1220 |
| | I | 0.940 | 129.2 | 63 | 55 | 8 | 755 |
| MPE2 | II | 0.947 | 130.5 | 68 | 59 | 9 | 840 |
| | III | 0.952 | 131.7 | 71 | 60 | 11 | 852 |
| | I | 0.936 | 124.4 | 61 | 44 | 17 | 539 |
| MPE3 | II | 0.943 | 125.6 | 65 | 52 | 13 | 740 |
| | III | 0.947 | 128.6 | 68 | 56 | 12 | 884 |
| | I | 0.948 | 128.1 | 69 | 58 | 11 | 970 |
| ZNPE1 | II | 0.957 | 129.0 | 74 | 59 | 15 | 1161 |
| | III | 0.964 | 131.2 | 78 | 65 | 13 | 1462 |
| | I | 0.920 | 121.4 | 50 | 30 | 20 | 224 |
| ZNPE2 | II | 0.924 | 122.0 | 52 | 30 | 22 | 283 |
| | III | 0.926 | 127.5 | 54 | 31 | 23 | 329 |

[a] Melting temperature of the strongest peak in treatment mode III at a heating rate of 10°C/min.

dence suggests that a third phase exists, i.e., a partially ordered interfacial phase, in semicrystalline polymers. Mandelkern et al.[25] believed that the difference between the crystallinity obtained from density and fusion enthalpy were primarily due to interfacial contributions. They found that:

$$\chi_d > \chi_{\Delta H} \tag{3}$$

$$\alpha_c \approx \chi_{\Delta H} \tag{4}$$

$$\alpha_c + \alpha_i = 1 - \alpha_a \approx \chi_d \tag{5}$$

where $\alpha_c$, $\alpha_a$, and $\alpha_i$ are the fractions of chain units in the perfect crystal, in the amorphous phase and in the partially ordered interfacial region, respectively.

The $\chi_d$, $\chi_{\Delta H}$, and estimated content of the interfacial region ($\alpha_i$) are summarized in Table II. The values $\chi_d$ of are indeed larger than the values of $\chi_{\Delta H}$, and the differences between them decrease with increasing in crystallinity (Fig. 4), indicating that there is less interfacial phase in polymers of higher crystallinity.[26] Comparing the crystallinity of MPE1 and ZNPE1, it can be seen that they have close crystallinity from density, because the densities of them are similar. However, a small difference is found for the crystallinity from fusion enthalpy in treatment models II and III; thus, ZNPE1 has a little more interfacial region than MPE1. The formation of the interfacial phase is mainly due to the irregular folding of the polymer chains, such as nonadjacent reentry,[27] which is related to the distribution of comonomer units along the polymer chains. Therefore, the less content of the interfacial region implies a more homogeneous intramolecular composition distribution in metallocene-based ethylene copolymers.

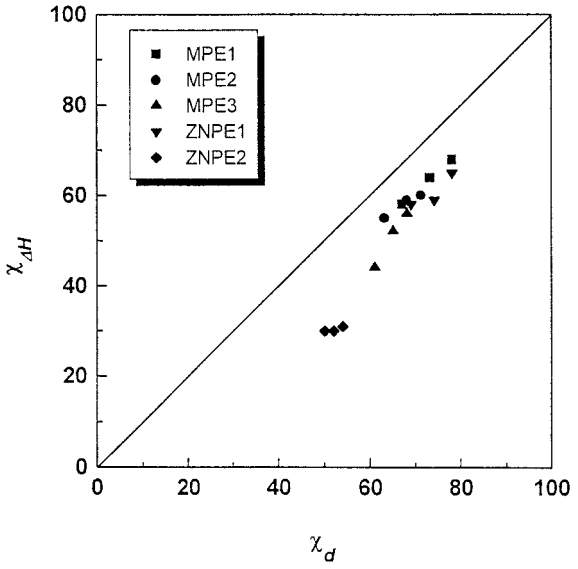


**Figure 4** The differences between crystallinity from density and from fusion enthalpy.

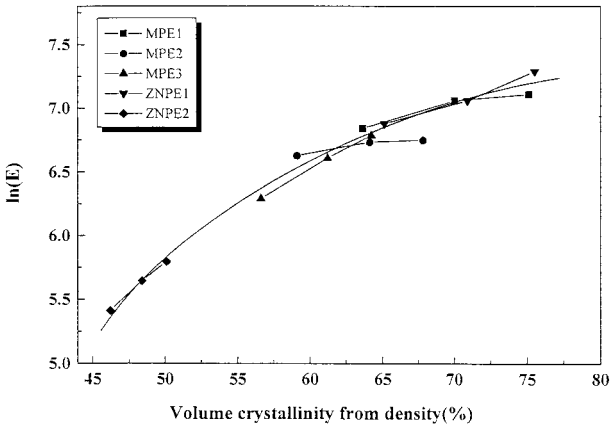


**Figure 5** Initial modulus of different samples.

### Initial Modulus

The data of the initial modulus for all samples are also given in Table II. Figure 5 is the plot of the initial modulus against the volume fraction crystallinity from the density. All data can approximately be fitted by a single curve, which shows that modulus increases rapidly with crystallinity in the low crystallinity region but slowly in the high crystallinity region.

However, a subtle difference among these samples is also appreciable. The modulus of MPE1 and MPE2 is nearly keep constant from treatment models II to III despite the increase in crystallinity, while the modulus of other samples increases continuously. This difference should not be attributed to experimental error, because it occurs in two polymer having the narrowest SCBD simultaneously. This probably results from the difference in SCBD. To further verify this idea, we can examine the initial modulus of MPE1 and ZNPE1, which has similar density at any treatment mode. It is observed that they have close initial modulus under both treatment procedures I and II. Sehanobish et al.[28] also found that composition distribution has little effect on modulus of the ethylene copolymers. However, in treatment model III, these two samples show a distinct difference in initial modulus, and ZNPE1 has a larger modulus than MPE1 when crystallized stepwise. These phenomena suggest that SCBD has some effect on the initial modulus of ethylene copolymers, but this effect is only observable under some special conditions.

This influence of SCBD on the initial modulus may take effect through its effect on the morphology of the polymer. Mandelkern et al.[29] found that spherulites were observed in quenched ethylene homopolymers or annealed at lower temperature, while only rod-like crystals appeared when PE was annealed at a higher temperature. A preliminary study of polarized light microscopy (PLM) in our work also showed that spherulites, which were the basic morphology of all samples treated in the I and II modes, were not observed in the stepwise crystallized samples.

The semicrystalline polymer can be viewed as a composite composed of amorphous matrix and crystals as rigid fibers (filler). This system was treated as randomly oriented piles that individually are unidirectional short-fiber composites, and the modulus of the semicrystalline composite with the $b$-axis of the crystal oriented in the tensile direction was obtained as follows:[30,31]

$$E = \frac{E_a[E_c + \xi(\alpha E_c + (1 - \alpha)E_a)]}{\alpha E_c + (1 - \alpha)E_a + \xi E_a} \quad (6)$$

In eq. (6), $\alpha$ is the volume fraction crystallinity and $\xi$ is the crystal aspect ratio-dependent parameter, and is equal to $2(L/D)$, i.e., two times the ratio of the length or width of the lamellar fiber and lamellar thickness. For spherulite crystals, the values of $\xi$ are identical for all samples, irrespectively of their size, and the initial modulus is a simple function of crystallinity. When the crystals exist in the other form instead of spherulites, the values of $\xi$ differ in shape, and the initial modulus also varies with $\xi$. In treatment mode III, SCBD may influence the $\xi$ value of rod-like crystals, leading to the different change trends of the initial modulus.

This work was financially supported by the National Natural Science Foundation of China (Grant No.: 59703002), and the State Key Laboratory of Polymeric Materials Engineering, CUST.

## REFERENCES

1. Hosoda, S.; Uemura, A. Polym J 1992, 24, 939.
2. Wooster, J. J.; Parikh, D. R.; Sehanobish, K.; Chum, S. P. Polym Prepr 1989, 30, 323.
3. Kennedy, M. A.; Peacock, A. J.; Mandelkern, L. Macromolecules 1994, 27, 5297.
4. Gaucher-Miri, V.; Elkoun, S.; Seguela, R. Polym Eng Sci 1997, 37, 1672.
5. Ward, I. M. Polym Eng Sci 1984, 24, 724.
6. Seguela, R.; Rietsch, F. Polymer 1986, 27, 703.
7. Seguela, R.; Rietsch, F. J Mater Sci 1988, 23, 415.

8. Sinn, H.; Kaminsky, W.; Vollmer, H. J.; Woldt, R. Angew Chem Int Ed Engl 1980, 19, 390.
9. Reddy, S. S.; Sivaram, S. Prog Polym Sci 1995, 20, 309.
10. Wild, L.; Ryle, T. R.; Knobeloch, D. C.; Peats, I. R. J Polym Sci Part B Polym Phys 1982, 20, 441.
11. Keating, M. Y.; McCord, E. F. Thermochim Acta 1994, 243, 129.
12. Liu, T. M.; Harrison, I. R. Thermochim Acta 1994, 233, 167.
13. Wlochowicz, A.; Eder, M. Polymer 1984, 25, 1268.
14. Hosemann, R.; Calleja, F. J. B. Polymer 1979, 20, 1091.
15. Karoglanian, S. A.; Harrison, I. R. Thermochim Acta 1992, 212, 143.
16. Karbashewski, E.; Kale, L.; Rudin, A.; Tschir, W. J.; Cook, D. G.; Pronovost, J. O. J Appl Polym Sci 1992, 44, 425.
17. Li, Y. M. Polymer Physics Experiments; Zhejiang University Press: China, 1993.
18. Chiang, R.; Flory, P. J. J Am Chem Soc 1961, 83, 2087.
19. Wunderlich, B. Macromolecular Physics, vol. 3. Crystal Melting; Academic Press, New York, 1980.
20. Xu, J. T.; Xu, X. R.; Feng, L. X.; Chen, W. Eur Polym J 2000, 36, 685.
21. Wild, L. Adv Polym Sci 1990, 98, 1.
22. Hosoda, S. Polym J 1988, 5, 383.
23. Kashiwa, N. Metcon'93 1993, 235.
24. Mandelkern, L. Polym J 1985, 17, 337.
25. Peacock, A. J.; Mandelkern, L. J Polym Sci Part B Polym Phys 1990, 28, 1917.
26. Fatou, J. G.; Macia, I. G.; Marco, C.; Gomez, M. A.; Arribas, J. M.; Fontecha, A.; Aroca, M.; Martinez, M. C. J Mater Sci 1996, 31, 3095.
27. Mandelkern, L. Acc Chem Res 1990, 23, 380.
28. Sehanobish, K.; Patel, R. M.; Croft, B. A.; Chum, S. P.; Kao, C. I. J Appl Polym Sci 1994, 51, 887.
29. Maxfield, J.; Mandelkern, L. Macromolecules 1977, 10, 1141.
30. Halpin, J. C.; Kardos, J. D. J Appl Phys 1972, 43, 2236.
31. Crist, B.; Fisher, C. J.; Howard, P. R. Macromolecules 1980, 22, 1709.